Electronic Supplementary Information

Covalent organic framework with self-contained light source for antitumor photodynamic therapy

Wen-Xiu Ren‡, Fei Kong ‡, Yu-Qing Shao, Qing-Yun Huang, Long-Fei Sun, Jie Feng*, Yu-Bin Dong*

College of Chemistry, Chemical Engineering and Materials Science, Collaborative Innovation Center of Functionalized Probes for Chemical Imaging in Universities of Shandong, Key Laboratory of Molecular and Nano Probes, Ministry of Education Shandong Normal University, Jinan 250014, People's Republic of China,

E-mail: Jiefeng@sdnu.edu.cn, yubindong@sdnu.edu.cn

Table of Contents

Experimental Section

1. Materials and Instruments

Materials: All reagents are analytically pure and used directly without further purification. N, N-Dimethylformamide (DMF), glacial acetic acid, ethanol, methanol dichloromethane and $FeCl_2 \cdot 4H_2O$ were purchased from Sinopharm Chemical Reagent Co., Ltd., o-dichlorobenzene and dimethyl sulfoxide (DMSO) were purchased from Shanghai Macklin Biochemical Co., Ltd., 5,10,15,20-tetra(4-aminophenyl) porphyrin was purchased from Jilin Yanshen Technology Co., Ltd., 2,5-dihydroxyterephthalaldehyde was purchased from ArK Pharm, Inc (Chicago, USA). Luminol was purchased from Aladdin Reagent Co., Ltd. Singlet Oxygen Sensor Green (SOSG) was purchased from Shanghai Maokang Biotechnology Co., Ltd. Active oxygen detection kit (DCFH-DA) were purchased from Shanghai Biyuntian Biotechnology Co., Ltd. 9,10-anthracenediyl-bis (methylene) dimalonic acid (ABDA) was purchased from Sigma-Aldrich (Shanghai) Trading Co. Ltd. (4,5-dimethyl-2-thiazolyl)-2,5-diphenyl-2-H-tetrazolium bromide (MTT) was purchased from Sigma-Aldrich (Shanghai) Trading Co. Ltd. Living dead cell staining kit (calcein-AM, PI) was purchased from Shanghai Yisheng Biotechnology Co., Ltd. 4% formaldehyde universal tissue fixative was purchased from Biosharp Co., Ltd. Dulbecco's Phosphate-Buffered Saline (DPBS), and Fetal Bovine Serum (FBS) were purchased from Biological Industries USA, RPMI Medium Modified (1640), Penicillin Streptomycin Mixtures (Pen-Strep), and Trypsin-EDTA Solution (0.25%) were purchased from HyClone Laboratories. Mouse breast cancer (4T1) cells, Human colorectal cancer (HCT116) cells and human breast adenocarcinoma (MCF-7) cells, which were purchased from the Procell Life Science & Technology Co., Ltd.

Instrument: Ultraviolet–visible (UV−vis) absorption spectra were recorded on a Shimadzu UV-2700 Double Beam UV−vis Spectrophotometer. Scanning electron microscopy (SEM) micrographs were recorded on a Hitachi SU8010 Scanning Electron Microscope. Transmission electron microscope (TEM) micrographs were recorded on a Hitachi HT7700 120kV Compact-Digital Transmission Electron Microscope. Powder X-ray diffraction (PXRD) patterns were obtained on a Rigaku Smart Lab SE X-Ray Powder Diffractometer with Cu Kα line focused radiation (λ = 1.5405 Å) from 2θ = 2.00° up to 50.00° with 0.01° increment. Fourier transform infrared (FT-IR) spectra were obtained in the 4000-400 cm^{-1} range using a Thermo Scientific Nicolet iS50 FT-IR Spectrometer equipped with diamond attenuated total reflection (ATR) module. Each spectrum was the average of 16 scans. Nitrogen adsorption isotherms were measured at 77 K with KUBO-X1000 aperture specific surface area analyzer. Hydrodynamic particle size and zeta potential were measured using Malvern Zetasizer Nano ZS90 System. Inductively coupled plasma (ICP) measurements were obtained on Thermo Scientific iCAP 7000 ICP-OES. Laser scanning confocal fluorescence images were captured with a Leica TCS SP8 Confocal Laser Scanning Microscopy with an objective lens (×20). The fluorescence images of the cells were performed on a confocal laser scanning microscope (TCS SP8, Leica, Wetzlar, Germany) with a pointed excitation wavelength. Cell proliferation data were obtained by Full-wavelength, multi-channel microporous plate detector-SpectraMax 190 optical absorption marker. Thermogravimetric analysis (TGA) was obtained by Mettler Toledo TGA2 thermogravimetric analyzer. All fluorescence measurements were performed on an F-4600 spectrofluorometer (Hitachi, Japan) equipped with a circulating water bath for temperature control. X-ray photoelectron spectroscopy (XPS) was performed using an ESCALAB 250 X-ray photoelectron spectrometer with a monochromatized Al Kα X-ray source (1486.71 eV). Chemiluminescence intensity was performed using Promega Glomax 96 microplate luminescence detector.

2. Synthesis of Fe-Tph, DhaTph, **Fe-DhaTph** and **Lum-in-Fe-DhaTph**

Synthesis of Fe-Tph. Fe-Tph was prepared by slightly modified method according to a literature method.[1] A mixture of 5,10,15,20-tetra(4-aminophenyl) porphyrin (20.24 mg, 0.03 mmol) and $FeCl_2 \cdot 4H_2O$ (29.82 mg, 0.15 mmol) in DMF (100 mL) was heated at 120 °C for 4 h. After cooling to room temperature, the resulting precipitate was collected, and completely washed three times with 1M HCl and deionized water, and dried in vacuum to afford Fe-Tph in 72% yield. FT-IR (ATR, cm^{-1}): 3346(m), 3204(w), 2961(w), 2922(w), 2851(w), 1652(w), 1601(s), 1510(w),

1488(w),1405(w), 1333(w), 1288(w), 1261(m), 1203(w), 1178(m), 1092(m), 1026(w), 999(m), 843(w), 801(s), 719(w), 571(w), 525(w), 428(w); MS (HR-MS) calcd for $C_{44}H_{32}ClFeN_8$: 764.0408, found: 764.5608.

Synthesis of DhaTph. DhaTph was synthesized according to the reported literature.[2, 3] A mixture of 2,5-dihydroxyterephthalaldehyde (Dha) (13.3 mg, 0.08 mmol), tetra(*p*amino-phenyl)porphyrin (Tph) (27.0 mg, 0.04 mmol), and acetic acid (0.2 mL, 6 M) in dichlorobenzene/ethanol (2 mL, 1:1) was ultrasonically treated for 10-15 minutes to obtain a uniform dispersion solution. Then the test tube was quickly frozen at 77K (liquid N_2 tank), degassed through three freeze-pump-thaw cycles, sealed, and heated at 120 °C for 3 days. Finally, the obtained solids were filtered out, completely washed with ethanol, and dried under vacuum at 150 °C for 12 hours. Yield, 74%. The characterization data are well consistent with the reported data. [2]

Synthesis of Fe-DhaTph. A mixture of Dha (13.3 mg, 0.08 mmol), Fe-Tph (9.5 mg, 0.013 mmol), Tph (18.225 mg, 0.017 mmol) and acetic acid (0.2 mL, 6 M) in dichlorobenzene/ethanol (2 mL, 1:1) was ultrasonically treated for 10-15 minutes to obtain a uniform dispersion solution. Afterward, the test tube was quickly frozen at 77K (liquid N_2 tank), degassed through three freeze-pump-thaw cycles, sealed, and heated at 120 °C for 5 days. Finally, the **Fe-DhaTph** powders were filtered out, completely washed with ethanol, and dried in vacuum at 150 °C for 12 hours. Yield, 68%. FT-IR (ATR, cm^{-1}): 3310(w), 3029(w), 2963(w), 2869(w), 1666(w), 1614(s), 1589(s), 1492(m), 1472(w), 1400(w), 1336(m), 1312(m), 1213(m), 1152(s), 1016(w), 999(w), 966(m), 889(w), 872(w), 851(w), 796(m), 735(w), 569(w), 483(w). The doped amount of Fe was determined as 1.43 wt% based on ICP-MS measurement.

Synthesis of Lum-in-Fe-DhaTph. A mixture of **Fe-DhaTph** (30 mg) and luminol (25 mg, 0.14 mmol) in 20 mL of $MeOH/CH_2Cl_2$ (8:2) was refluxed for 1 hour. After cooling to room temperature, the resulted solids were collected by centrifugation, washed by ethanol until the supreme liquid is colorless and then dried under vacuum. FT-IR (ATR, cm^{-1}): 3473(w), 3418(m), 3326(w), 2914(m), 1658(s), 1614(m), 1595(m), 1493(s), 1448(m), 1383(w), 1321(s), 1295(m), 1245(w), 1205(w), 1173(w), 1153(w), 1098(w), 1051(w), 999(m), 952(w), 852(w), 811(m), 786(w), 774(w), 700(m), 635(w), 531(w), 490(w). The loading capacity of luminol on **Lum-in-Fe-DhaTph** was calculated to be 40% (w/w) based on the standard curve by UV–vis spectroscopy.

3. Determination of the fluorescence quantum yield and CRET efficiency.

The relative quantum yield was measured by reference method.[4] Rhodamine B is widely used as a quantum yield standard due to its high molar extinction coefficient, high fluorescence quantum yield and good stability. The fluorescence quantum yield of rhodamine B in aqueous solution is 0.31. An aqueous solution of rhodamine B at an appropriate concentration was prepared, and its ultraviolet spectrum was measured. The absorbance (A_{st}) of rhodamine B at 415 nm was recorded to ensure that the A_{st} was less than 0.05. Then, the fluorescence emission spectra in the range of 440-800 nm were obtained with 415 nm as excitation wavelength, and the fluorescence integral peak area (S_{st}) was recorded. Similarly, **Fe-DhaTph** and **Lum-in-Fe-DhaTph** solutions with a certain concentration were prepared, and the above steps were repeated to record their absorbance (A_x) and fluorescence integral peak area (S_x). Substitute the above values into the following formula to calculate the quantum yields of **Fe-DhaTph** and **Lum-in-Fe-DhaTph.** η is the refractive index of the solvent used.

$$\Phi_x = \Phi_{st}\left(\frac{D_x}{D_{st}}\right)\left(\frac{A_{st}}{A_x}\right)\left(\frac{\eta_x^2}{\eta_{st}^2}\right)$$

The CRET efficiency was determined according to the literature method[4] to be ca. 14.29% by dividing the integral area of the **Fe-DhaTph** emission spectrum by the integral area of the whole spectrum of the **Lum-in-Fe-DhaTph**.

4. Photodynamic behavior of **Lum-in-Fe-DhaTph**

Singlet oxygen ($^1O_2$) detection. The $^1O_2$ generation of **Lum-in-Fe-DhaTph** was detected by 9,10-anthracenediyl-bis (methylene) dimalonic acid (ABDA), which can react with $^1O_2$ to produce endoperoxide and result in a decrease in the absorption intensity of itself. First, a total of 500 μL of

Lum-in-Fe-DhaTph (200 μg/mL) was mixed with 50 μL ABDA (10 mM) and 100 μL of H_2O_2 (100 mM). Next, the absorption intensity of the mixture solution was recorded by UV-vis spectrum at different intervals (0, 5, 10, 20, 40, 60, 80, 100, 120 min). In addition, **Lum-in-Fe-DhaTph** (200 μg/mL) without H_2O_2 was used as the control group. The generation of $^1O_2$ ability was also investigated in group of ABDA, ABDA with Fe^{3+} and H_2O_2, which was carried out under the same conditions as above.

5. Confocal imaging

Intracellular production of singlet oxygen ($^1O_2$) detection. MCF-7 cells were seeded in a confocal dish and incubated at a humidified incubator in 5% CO_2/95% air at 37 °C for 24 h. Then, the cell medium was replaced by the fresh culture medium containing **Lum-in-Fe-DhaTph** (200 μg/mL), incubated for additional 4 h. After removed the cell medium containing **Lum-in-Fe-DhaTph**, the cells were incubated with a singlet oxygen probe, singlet oxygen sensor green (SOSG), for additional 15 min at 37 °C. Afterwards, the cells were imaged by the confocal laser microscope at 488 nm excitation. In addition, the cells without any treatment, treated with **Fe-DhaTph** (120 μg/mL) or luminol (80 μg/mL), was used as a control to further evaluate the ability of $^1O_2$ generation. This control experiment is carried out under the same conditions as above.

Intracellular production of reactive oxygen species (ROS). MCF-7 cells were seeded in a confocal dish and incubated at a humidified incubator in 5% CO_2/95% air at 37 °C for 24 h. Then, the cell medium was replaced by the fresh cell medium containing **Lum-in-Fe-DhaTph** (200 μg/mL), and incubated for additional 4 h. After removed the cell medium containing **Lum-in-Fe-DhaTph**, the cells were incubated with a ROS probe, 2,7-dichlorodihydrofluorescein diacetate (DCFH-DA), for additional 30 min at 37 °C. Afterwards, the cells were imaged by the confocal laser microscope at 488 nm excitation. In addition, the cells without any treatment, **Fe-DhaTph** (120 μg/mL) or luminol (80 μg/mL) were used as a control to further evaluate the ability of ROS generation. This control experiment is carried out under the same conditions as above.

Live/dead cells staining assays. Four groups of MCF-7 cells were seeded in confocal dishes and incubated at a humidified incubator in 5% CO_2/95% air at 37 °C for 24 h. Then, the four groups of cells were treated with **Fe-DhaTph** (120 μg/mL), luminol (80 μg/mL), and **Lum-in-Fe-DhaTph** (200 μg/mL), respectively. After cells were cultured for 24 h, the medium was removed and stained by the Calcein-AM (2 μM) and PI (4.5 μM) at 37 °C for 30 min. After being washed by PBS for three times, the cells were imaged by the confocal laser microscope at 488 nm excitation and 543 nm excitation, respectively.

6. MTT assays

Biocompatibility. To evaluate the biocompatible of **Fe-DhaTph**, 4T1, HCT116 and MCF-7 cells were separately seeded into 96-well plates and incubated at a humidified incubator in 5% CO_2/95% air at 37 °C for 24 h. Then the cells medium was replaced by the fresh cell medium containing different concentrations of **Fe-DhaTph** (0, 15, 30, 45, 60, 90, 120, 240 μg/mL), and incubated for additional 24 h. Afterwards, the cells medium was removed and the resulted cells were washed with PBS for three times. Then MTT (100 μL, 0.5 mg/mL) solution was added into each well. After incubated at 37 °C for four hours, the remaining MTT solution was removed and the DMSO (150 μL) was added to each well to dissolve the formazan crystals. The absorbance intensity at 490 nm was recorded by Microplate reader. Similarly, the biocompatible of luminol with different concentrations (0, 10, 20, 30, 40, 60, 80, 160 μg/mL) was investigated by the same method.

In vitro photodynamic effect. To investigate the photodynamic effect of the **Lum-in-Fe-DhaTph**, 4T1 cells were seeded in 96-well plates for overnight, and then 4T1 cells were incubated with **Lum-in-Fe-DhaTph** (0, 25, 50, 75, 100, 150, 200, 400 μg/mL) for additional 24 h. Afterwards, removed the cells medium and washed with PBS for three times, the cell viability was investigated by MTT assay using the method described in above. In addition, the group of cells without any treatment was used as a control to evaluate the photodynamic effect of the **Lum-in-Fe-DhaTph**. For HCT116 cells and MCF-7 cells, the operation procedure was the same as 4T1 cells.

7. Animal assays

Animal tumor xenograft models. Female BALB/c nude mice (aged 5~6 weeks, and 15~20 g body weight) purchased from the Beijing Vital River Laboratory Animal Technology Co., Ltd. (Beijing, China) were used for tumor xenograft establishment. Animal experiments were reviewed and approved by the Ethics Committee of Shandong Normal University, Jinan, P. R. China (approval number AEECSDNU2021041). All the animal experiments complied with relevant guidelines of the Chinese government and regulations for the care and use of experimental animals. Typically, each mouse was subcutaneous injected with 1×10^6 of living 4T1, HCT116 cells or MCF-7 cells dispersed in 70 μL of PBS. The injection sites were under the armpit of nude mice. When the tumor volume reached to approximately 60-70 mm^3, the following experiments were carried out.

Hemolytic test. Blood cells were obtained from the mice and incubated with different concentrations of **Lum-in-Fe-DhaTph** (0, 6.25, 12.5, 25, 50, 100, 150, 200, 400 μg/mL) for 4 h, where the PBS and pure water were separately used as negative and positive controls. Then, the samples were centrifuged at 4000 rpm for 5 min, and the supernatant were used for absorbance measurement by a Microplate reader.

In vivo antitumor photodynamic treatment. The 4T1, HCT116 or MCF-7 subcutaneous xenograft nude mice was randomly divided into three groups, including PBS, **Fe-DhaTph** and **Lum-in-Fe-DhaTph**. Concretely speaking, mice were intravenous injected with PBS**, Fe-DhaTph** nanoparticles and **Lum-in-Fe-DhaTph** with the dose of 100 μL, 240 μg/mL and 400 μg/mL every 3 days, respectively. The tumor volume and the weight of the nude mice were recorded every day. At the end of the treatment process, the mice were sacrificed and the major organs were collected for histological analysis. Specifically, these organs were fixed in 10% paraformaldehyde solution, and prepared to slices in process routinely. Then the slices were stained with hematoxylin and eosin, and observed by a confocal laser microscope.

Supplementary Figures

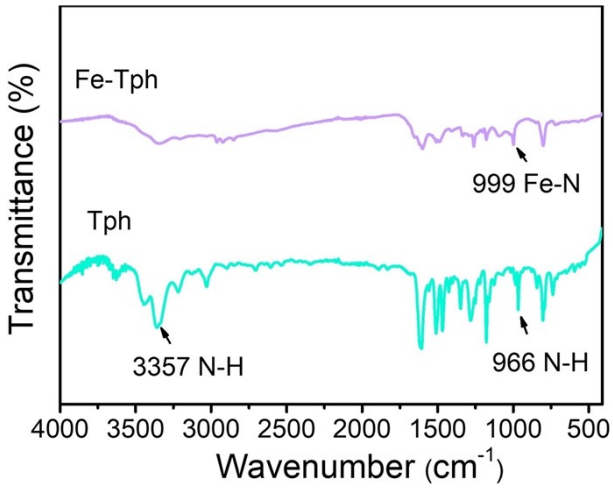

Fig. S1 FT-IR spectra of Tph and Fe-Tph. The characteristic band at 999 cm^{-1} associated with Fe-N clearly indicated the formation of Fe-Tph.

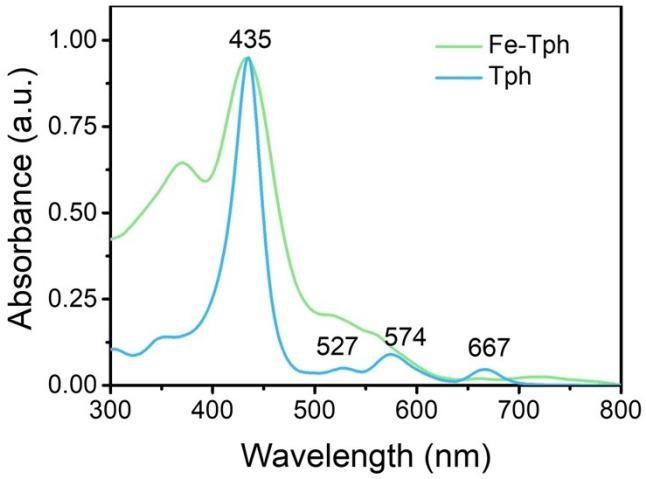

Fig. S2 UV-vis spectra of Tph and Fe-Tph. Tph has the Soret and Q bands at 435 nm and 527, 574 and 667 nm, respectively. The number of Q bands decreased after Fe ion doping, further confirming the formation of Fe-Tph.

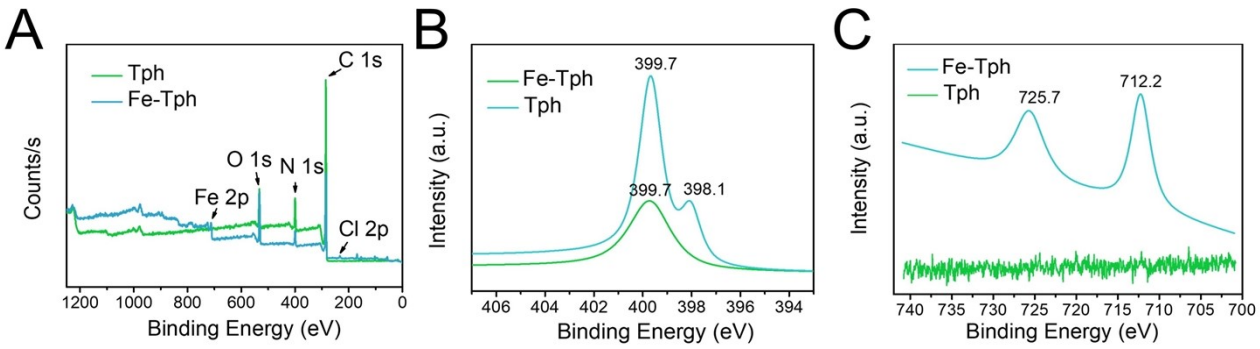

Fig. S3 XPS spectra of total spectrum of Tph and Fe-Tph (A). The XPS spectra showing the binding energy of N 1s (B) and Fe 2p (C) of Tph and Fe-Tph. The two peaks of Fe 2p at 725.7 and 712.2 eV indicated that the doped Fe is trivalent.

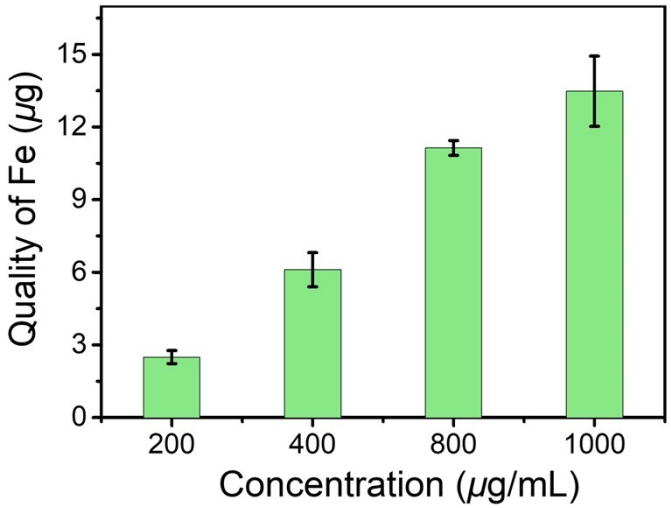

Fig. S4 Quantitative analysis of **Fe-DhaTph** with different concentrations by ICP-MS.

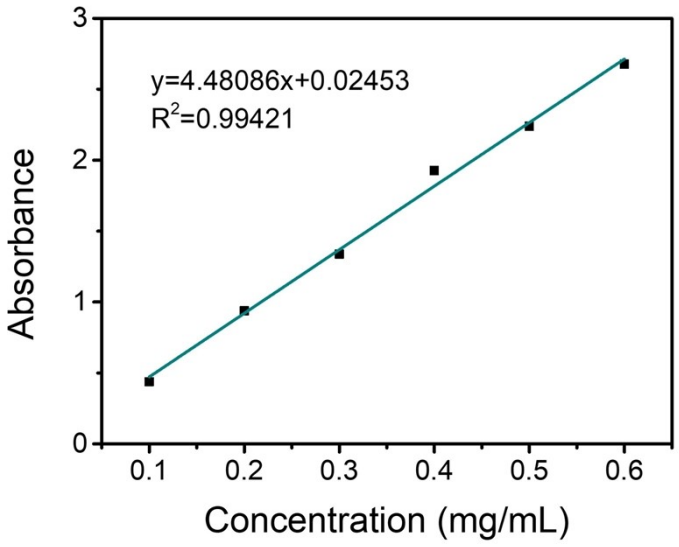

Fig. S5 Standard curve of luminol.

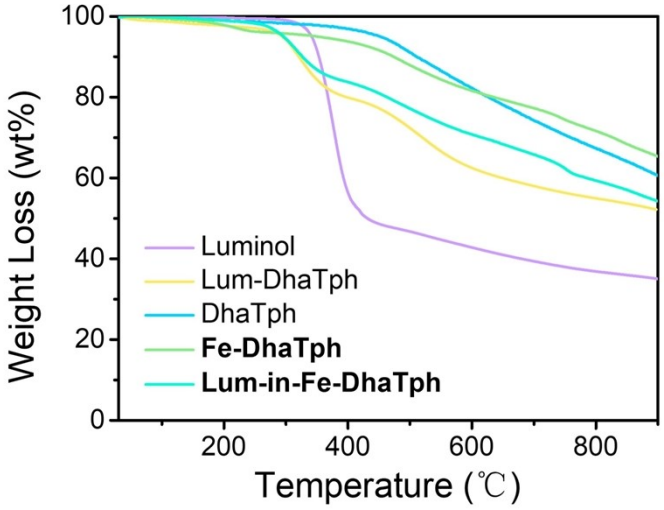

Fig. S6 TGA traces of luminol, Lum-DhaTph, DhaTph, **Fe-DhaTph** and **Lum-in-Fe-DhaTph** under N_2 atmosphere.

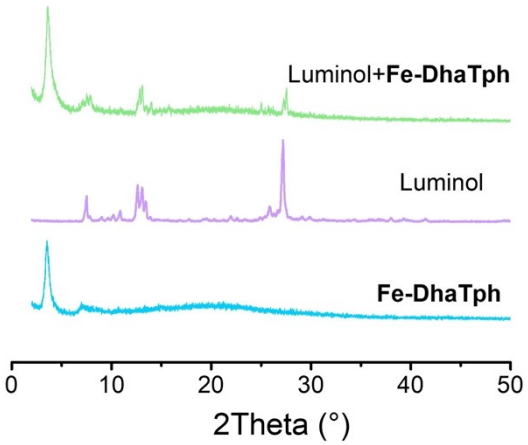

Fig. S7 PXRD pattern of **Fe-DhaTph**, luminol and Luminol + **Fe-DhaTph**. The "luminol + **Fe-DhaTph**" mixture was prepared by physically mixing of free luminol with **Fe-DhaTph.** It is different from **Lum-in-Fe-DhaTph**, the diffraction peaks belonging to luminol were clearly observed at 2θ = 7.61°, 7.82°, 12.84°, 13.06°, 13.51°, 13.96°, 27.53°.

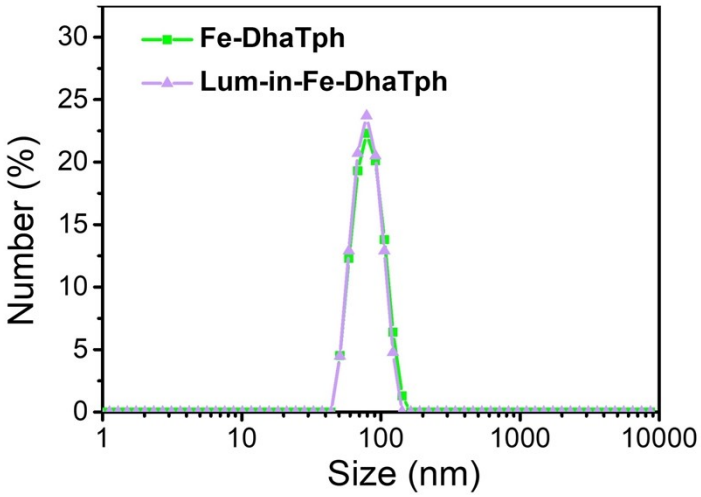

Fig. S8 Size distributions of **Fe-DhaTph** and **Lum-in-Fe-DhaTph** in PBS (pH = 7.4) at 25 °C.

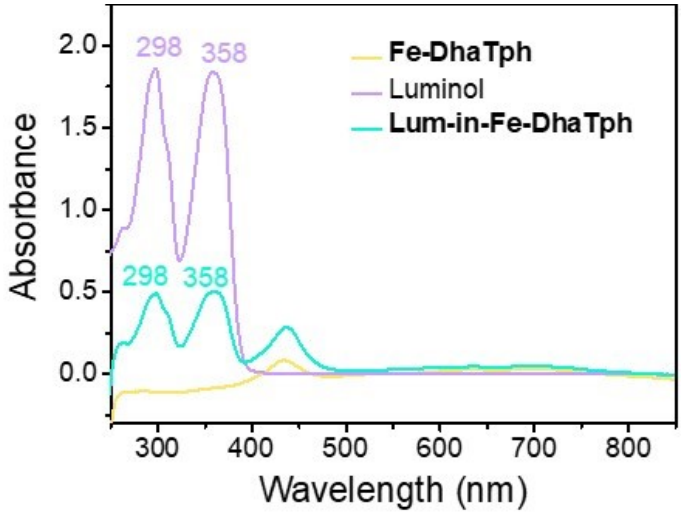

Fig. S9 UV-vis spectra of **Fe-DhaTph**, luminol and **Lum-in-Fe-DhaTph**.

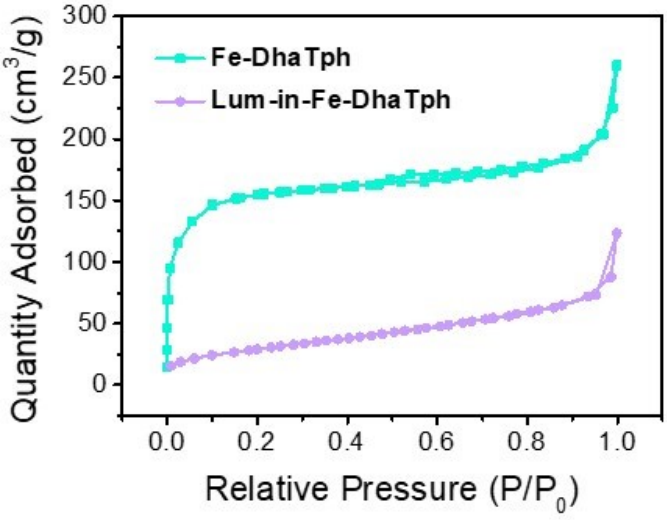

Fig. S10 N_2 adsorption and desorption isotherms at 77 K of **Fe-DhaTph** and **Lum-in-Fe-DhaTph**.

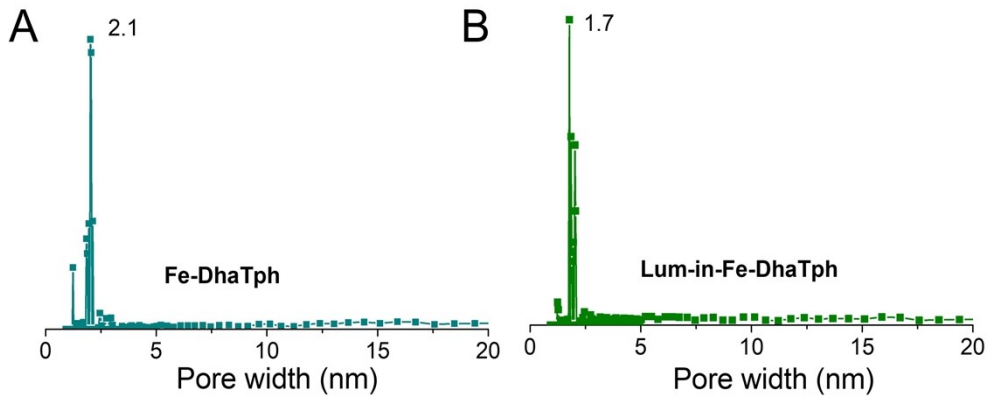

Fig. S11 Pore size distributions of **Fe-DhaTph** (A) and **Lum-in-Fe-DhaTph** (B) based on Barrett–Joyner–Halenda (BJH) model. After luminol loading, the pore size of **Fe-DhaTph** decreased from 2.1 to 1.7 nm in **Lum-in-Fe-DhaTph**.

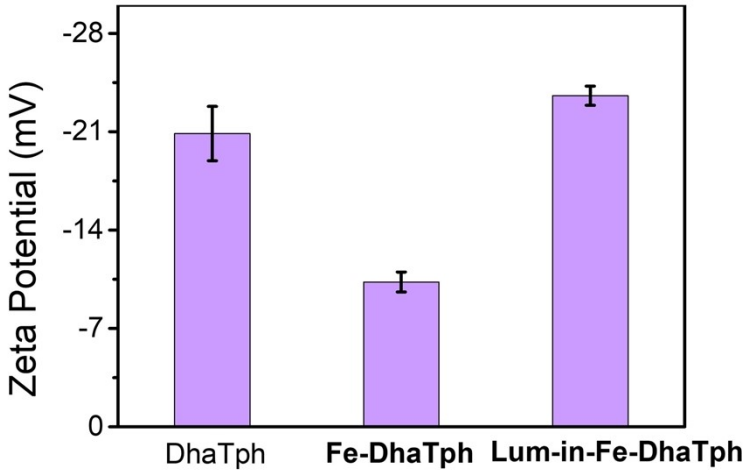

Fig. S12 Zeta potentials of DhaTph, **Fe-DhaTph** and **Lum-in-Fe-DhaTph** in PBS (pH 7.4).

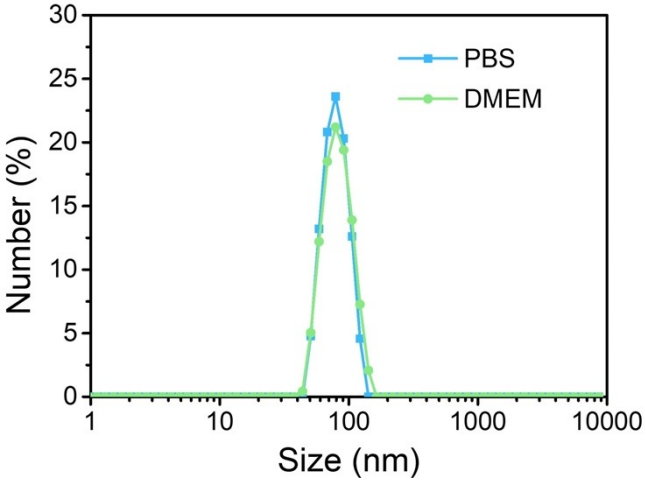

Fig. S13 Size distribution of **Lum-in-Fe-DhaTph** dispersed in PBS (size: 76.59 nm) and DMEM (size: 76.70 nm) after 24 h.

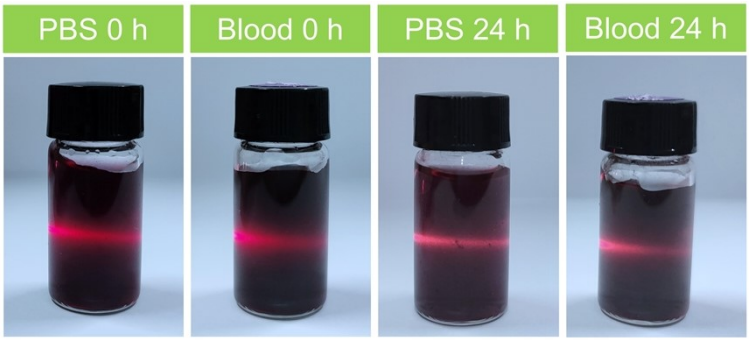

Fig. S14 Digital photographs of **Lum-in-Fe-DhaTph** in PBS and blood for 24 h under red laser irradiation. The observed Tyndall effect indicated that the PBS and blood dispersions of **Lum-in-Fe-DhaTph** are stable at least for 24 h.

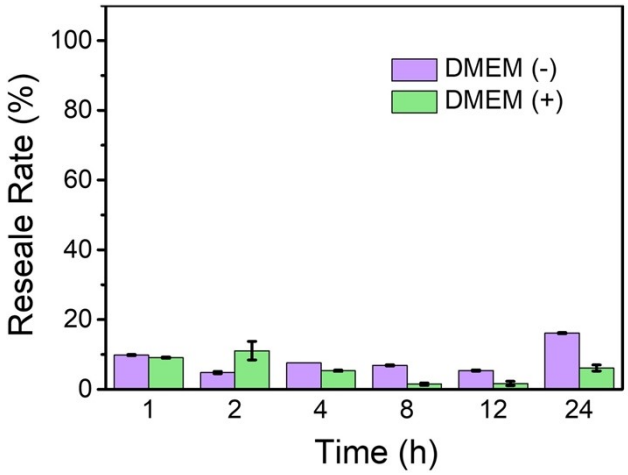

Fig. S15 Luminol release rate in DMEM (-) and DMEM (+) at different times.

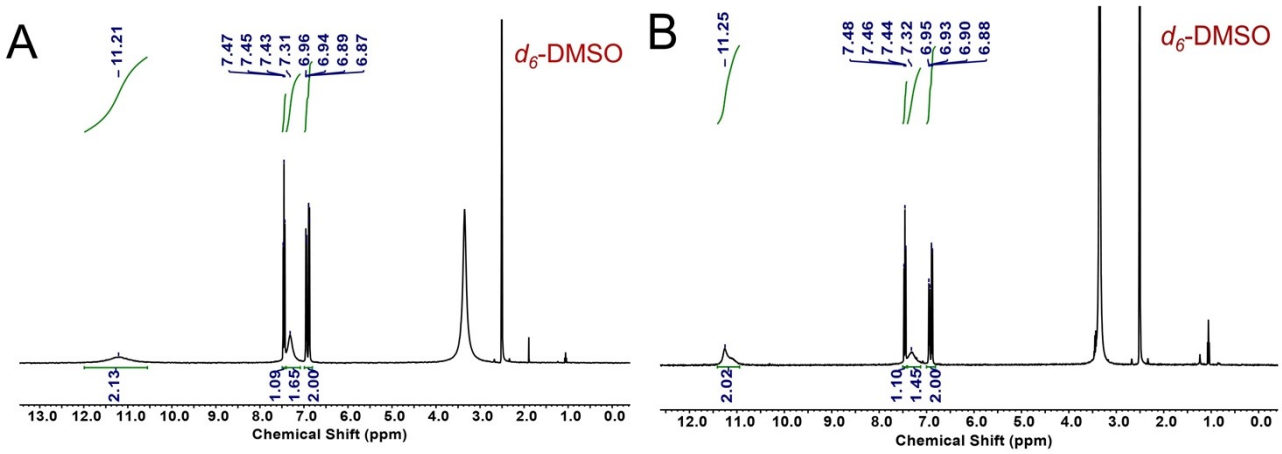

Fig. S16 ^{1}H NMR spectra of free luminol (A) and the DMSO-d_6 extract from the PBS solution of **Lum-in-Fe-DhaTph** after 24 h (B). As is shown, the encapsulated luminol is stable in **Lum-in-Fe-DhaTph** after it in PBS for 24 h.

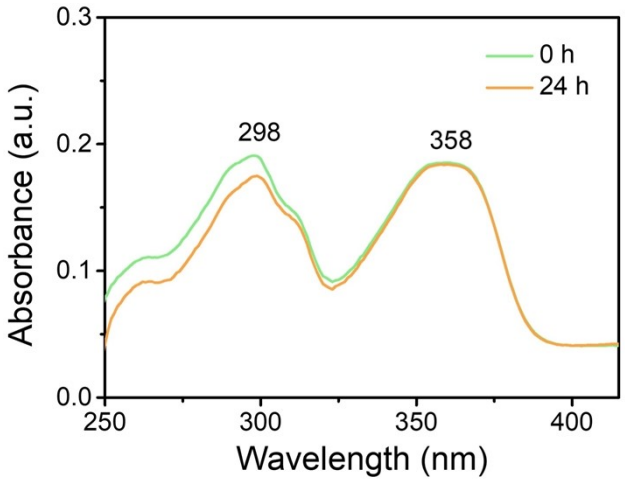

Fig. S17 UV spectra of luminol extracted from **Lum-in-Fe-DhaTph** (100 μg/mL) by DMSO before and after in PBS for 24 h. No adsorption change for luminol was found, indicating the encapsulated luminol is stable in **Lum-in-Fe-DhaTph** after it in PBS for 24 h.

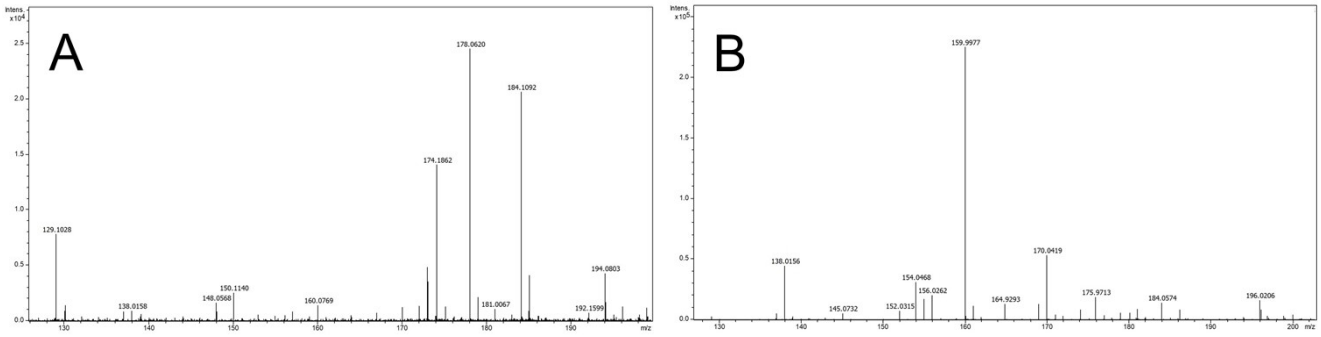

Fig. S18 (A) Mass spectrum of free luminol (calcd for $C_8H_7N_3O_2$: 178.0611, found: 178.0620). (B) Mass spectrum of the supernatant collected from the **Lum-in-Fe-DhaTph** in PBS for 24 h. No expected hydrolysis product of 3-aminophthalic acid (calcd for $C_8H_7NO_4$, 182.0448) was found.

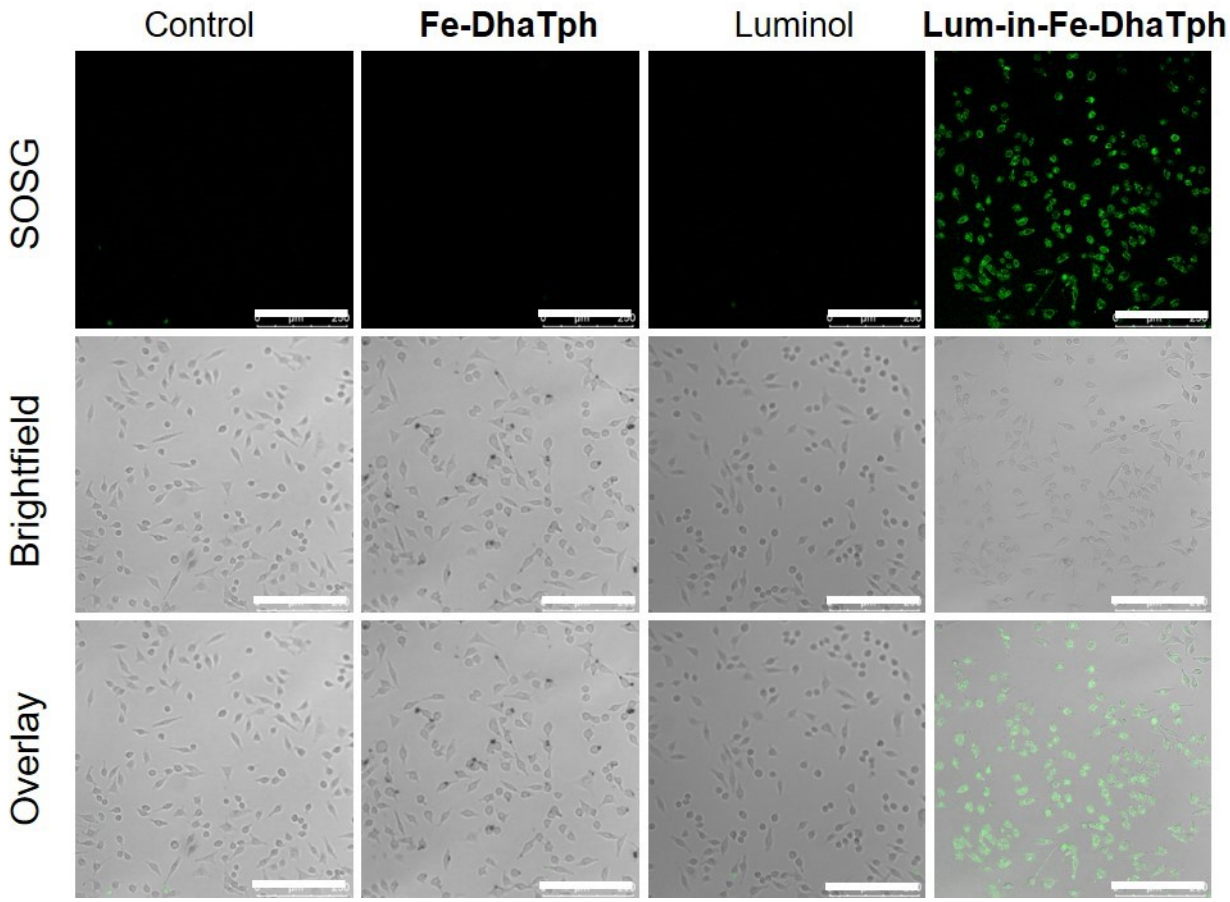

Fig. S19 Detection of intracellular $^1O_2$ using SOSG from intact MCF-7 cells, MCF-7 cells with **Fe-DhaTph** (120 μg/mL), Luminol (80 μg/mL), **Lum-in-Fe-DhaTph** (200 μg/mL), Scale bar, 250 μm.

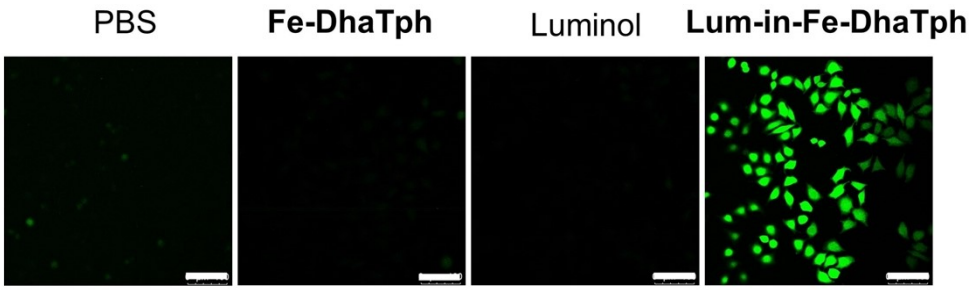

Fig. S20 CLSM images of intracellular ROS generation from intact MCF-7 cells, MCF-7 cells with **Fe-DhaTph** (120 μg/mL), luminol (80 μg/mL), **Lum-in-Fe-DhaTph** (200 μg/mL) respectively. Scale bar, 100 μm. As is shown, the intracellular CRET-mediated ROS generation of **Lum-in-Fe-DhaTph** was performed with 2,7-dichlorofluorescein diacetate (DCFH-DA) as the specific ROS probe. As a result, fluorescence signal was clearly detected in the **Lum-in-Fe-DhaTph** treated group due to the formation of highly fluorescent DCF in the presence of $^1O_2$. While no fluorescence was observed in the control groups, including pure PBS, **Fe-DhaTph** and free luminol groups.

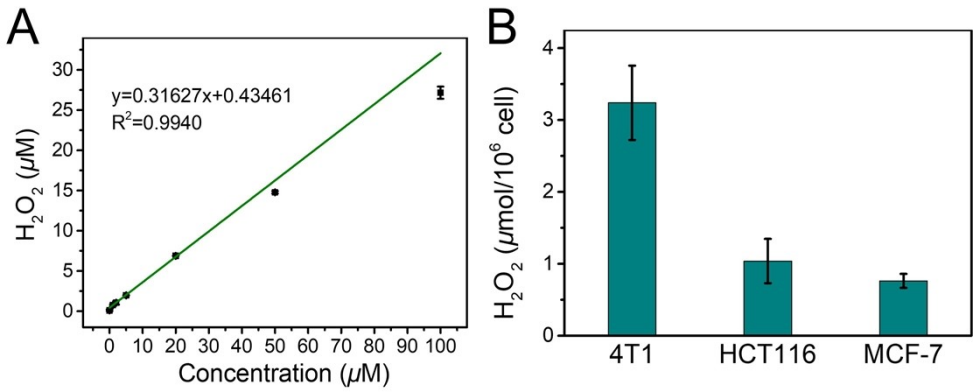

Fig. S21 Detection of intracellular H_2O_2 level. (A) Standard curve of H_2O_2. (B) Quantitative detection of intracellular H_2O_2 concentration of various cell lines based on cell number based on manufacturer's instructions.

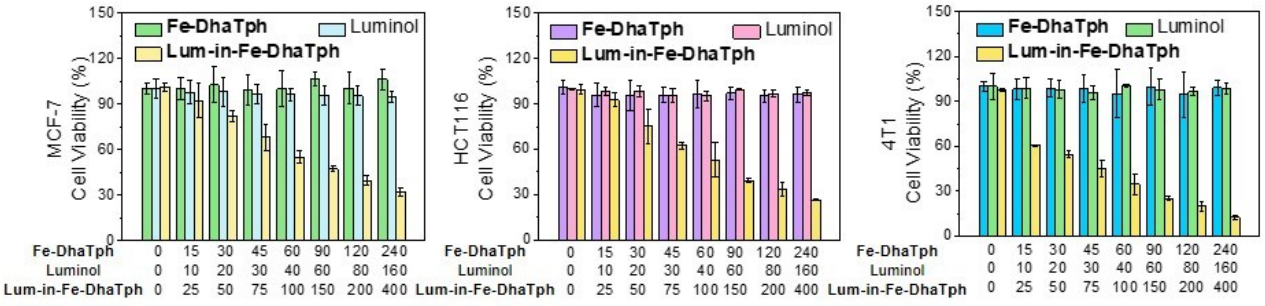

Fig. S22 MTT assay of MCF-7, HCT116 and 4T1 cells in the presence of different concentrations of **Fe-DhaTph**, luminol and **Lum-in-Fe-DhaTph**. For comparison, the cytotoxicity of Fe-DhaTph and luminol with the concentrations equivalent to **Lum-in-Fe-DhaTph** are also shown.

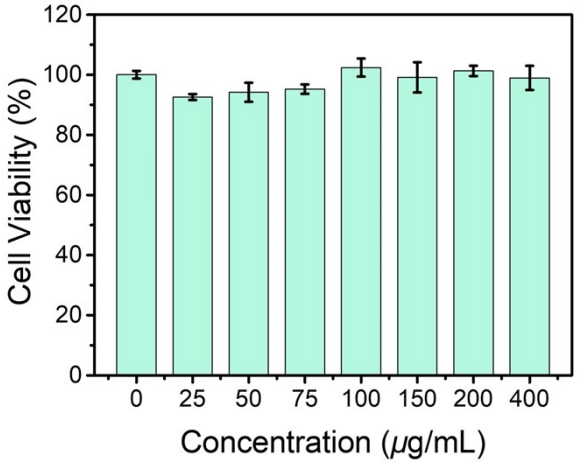

Fig. S23 MTT assay of MCF-10A cells in the presence of different concentrations of **Lum-in-Fe-DhaTph.** The normal cell lines were respectively incubated with different concentrations of **Lum-in-Fe-DhaTph** for 24 h. Negligible cell death was observed in all groups, revealing the good biocompatible of **Lum-in-Fe-DhaTph** towards normal cells.

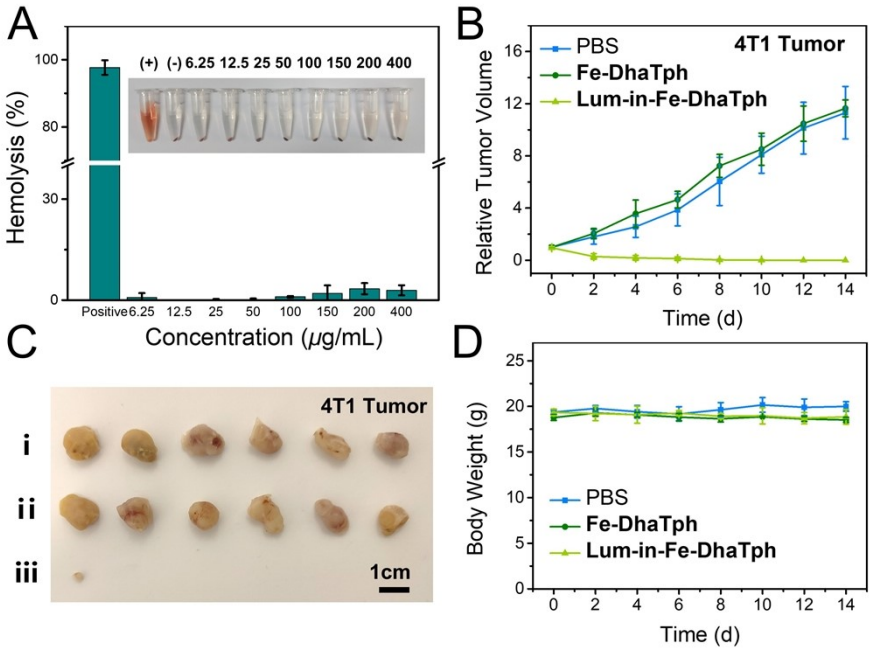

Fig. S24 Antitumor therapy in vivo. (A) Hemolytic assay using red blood cells incubated with control solvents and different concentrations of **Lum-in-Fe-DhaTph.** Inset: Hemolysis in red blood cells created by different treatment. Water and PBS were used as the positive and negative control, respectively. (B) Relative 4T1 tumor volume growth curves over time for the different groups from 0 to 14 days. (C) Photographs of 4T1 tumor tissues obtained after treatment (i, PBS-treated group; ii, **Fe-DhaTph**-treated group; iii, **Lum-in-Fe-DhaTph** -treated group). Scale bar, 1 cm. (D) Body weights of 4T1 tumor-bearing mice in different groups.

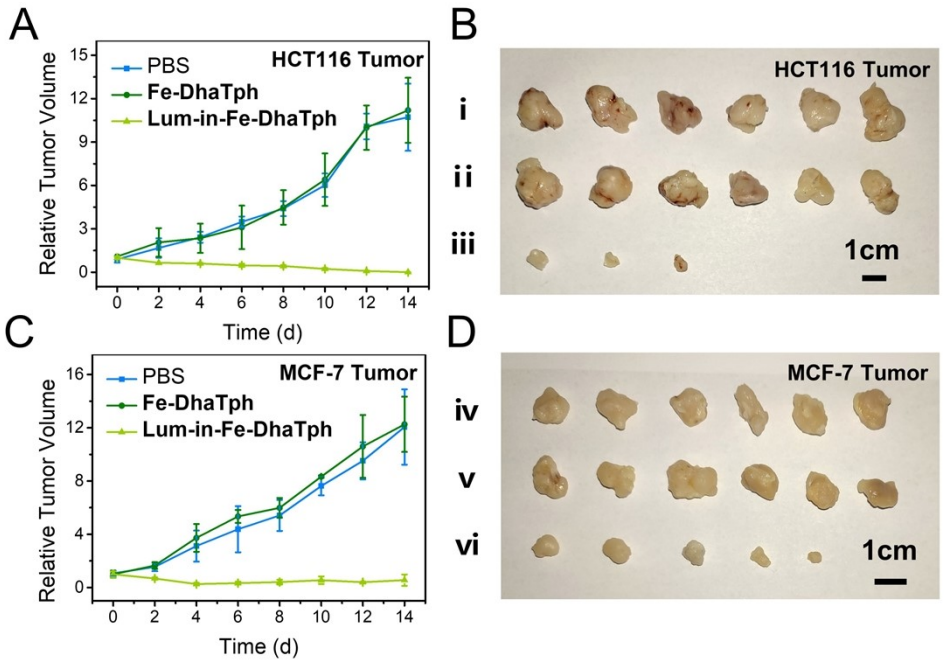

Fig. S25 Antitumor therapy in vivo. (A) Relative HCT116 tumor volume growth curves over time for the different groups from 0 to 14 days. (B) Photographs of HCT116 tumor tissues obtained after treatment (**i**, PBS treated group; **ii**, **Fe-DhaTph** treated group; **iii**, **Lum-in-Fe-DhaTph** treated group). Scale bar, 1 cm. (C) Relative MCF-7 tumor volume growth curves over time for the different groups from 0 to 14 days. (D) Photographs of MCF-7 tumor tissues obtained after treatment (**iv**, PBS treated group; **v**, **Fe-DhaTph** treated group; **vi**, **Lum-in-Fe-DhaTph** treated group). Scale bar, 1 cm. After the tumor volume increased to 60-70 mm^3, the mice were equally dived into three groups and treated with pointed administration. Groups **i** and **ii** were the control groups, which treated by PBS and **Fe-DhaTph**

respectively. Group **iii** was the treatment group, in which **Lum-in-Fe-DhaTph** dispersed in PBS and intravenous injected into the mice with 400 μg/mL dose of each mouse every three days. As shown in Figure S24A, for groups **i** and **ii**, the tumor volume increased rapidly as time went on. For the treatment group **iii**, the tumor growth was partly suppressed, and the tumor tissues on three of mice were ablated at the end of the treatment process (Figure S24B). For comparison, the antitumor efficiency of **Lum-in-Fe-DhaTph** for an MCF-7 xenograft model was also examined under the same treatment conditions. As shown in Figure S24C, D, when the lowest H_2O_2 expressed MCF-7 tumors were treated with **Lum-in-Fe-DhaTph**, a relatively poorer PDT efficacy was observed compared to the HCT116 xenograft under the same treatment conditions. This demonstrated that our **Lum-in-Fe-DhaTph** could serve as a potentially effective nanomedicine for CRET-mediated PDT, especially for those H_2O_2-high tumors. In addition, the excellent biosafety and biocompatibility of **Lum-in-Fe-DhaTph** were further proved by the body weights measurements (Figure S25) and H&E analysis (Figure S26).

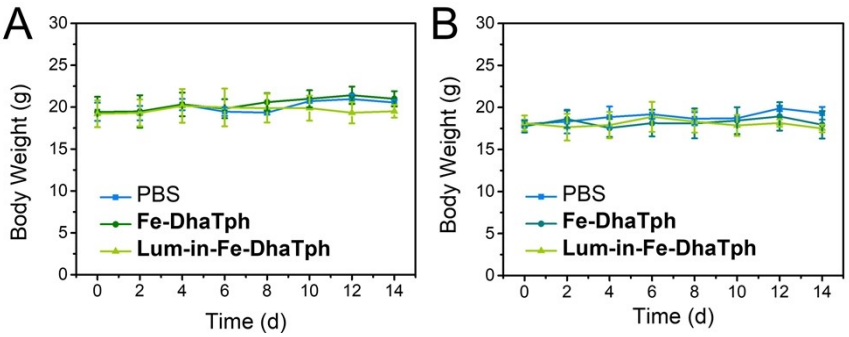

Fig. S26 Body weights of HCT116 tumor-bearing mice (A) and MCF-7 tumor-bearing mice (B) in different groups. All nude mice with intravenous injection presented a steady growth or no change in their body weight.

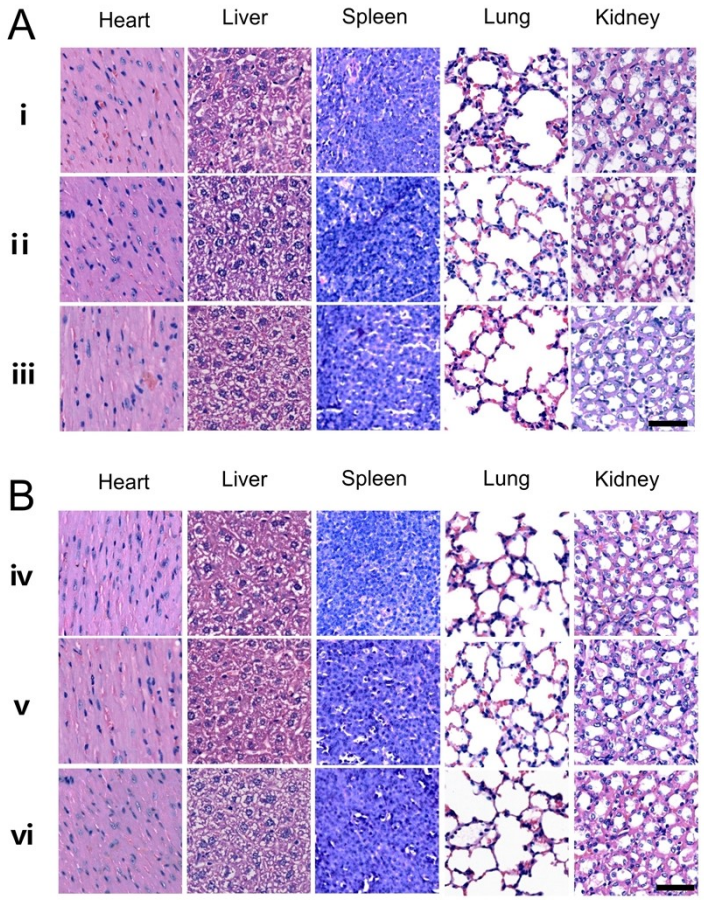

Fig. S27 Sections of major organs stained with H&E for HCT116 tumor-bearing mice (**i**, PBS treated group; **ii**, **Fe-DhaTph** treated group; **iii**, **Lum-in-Fe-DhaTph** treated group) (A) and MCF-7 tumor-bearing mice (**iv**, PBS treated group; **v**, **Fe-DhaTph** treated group; **vi**, **Lum-in-Fe-DhaTph** treated group) (B), Scale bar, 50 μm. There were no obvious pathological variations in each excised major organ, implying the laudable biocompatibility of the **Lum-in-Fe-DhaTph** nanocomposite.

References

1. M. Aghayan, A. Mahmoudi, K. Nazari, S. Dehghanpour, S. Sohrabi, M. R. Sazegar and N. M.-Tabrizi, *J. Porous Mater.,* 2019, **26**, 1507–1521.
2. S. Kandambeth, D. B. Shinde, M. K. Panda, B. Lukose, T. Heine and R. Banerjee, *Angew. Chem. Int. Ed.,* 2013, **52**, 13052-13056.
3. J. Feng, W.-X. Ren, F. Kong and Y.-B. Dong, *Chem. Commun.,* 2021, **57**, 7240-7243.
4. Z. Li, Y. Wang, G. Zhang, W. Xu, Y. Han, *J. Lumin.* 2010, **130**, 995-999.

Author Contributions

W.-X.R. and F.K contributed equally to this work.